International Journal of Pharmaceutics 374 (2009) 96–105

Contents lists available at ScienceDirect

International Journal of Pharmaceutics

journal homepage: www.elsevier.com/locate/ijpharm

# Role of drug substance material properties in the processibility and performance of a wet granulated product

Chandra Vemavarapu*, Madhu Surapaneni, Munir Hussain, Sherif Badawy

*Pharmaceutical Research & Development, Bristol-Myers Squibb Company, One Squibb Drive, New Brunswick, NJ 08903, USA*

ARTICLE INFO

*Article history:*
Received 6 August 2008
Received in revised form 12 February 2009
Accepted 12 March 2009
Available online 24 March 2009

*Keywords:*
High-shear wet granulation
Material properties
Granule growth
Compactability
Powder flow

ABSTRACT

The purpose of this study was to establish a relationship between the material properties of an active pharmaceutical ingredient (API) and its behavior during high-shear wet granulation. Using several actives and excipients as material probes, the influence of aqueous solubility, wettability, water holding capacity, mean and width of the particle size distribution, and surface area was examined. The effect of these variables on the processibility and performance of the granulations was evaluated by monitoring such responses as granule growth, compactability and flow changes upon wet granulation. The prominent findings from this study include: (a) controlled growth is highest in readily wettable APIs with low surface area, (b) uncontrolled growth is high in APIs of high solubility and low water holding capacity, (c) polydisperse granulations are produced from APIs of high contact angle and surface area, (d) improvement in compactability is high in APIs with large surface area and broader size distributions and (e) flow enhancement as a result of wet granulation is highest in APIs of large size distributions. These results are physically interpreted in this manuscript based on the prevailing wet granulation theories. Findings from this study are useful in mapping a new material to predict its performance in a high-shear wet granulation process.


## 1. Introduction

Organic drug substances are for the most part, fine, low density, cohesive powders that do not inherently lend themselves to subsequent handling and processing. Efforts are in vogue in the areas of crystal and particle engineering to build quality into the drug substances, primarily to improve their biopharmaceutical, physicochemical and mechanical properties (collectively called develop-ability of an active) (Lee and Myerson, 2006). Dosage form development conventionally relies on *granulation* as a means to build such quality into the drug product. Through size enlargement and some densification, granulation operation transforms fine actives into porous spherical structures. The substrate for such structures is commonly the diluent or the active, with a layer of binder coated around the primary particles. As a result, granulations exhibit improved flow, content uniformity and tablettability with reduced propensity for segregation, generation of airborne dust and electrostatic charge. All the abovementioned are important quality attributes from the standpoints of the manufacturer, regulatory agency and the patient (dosing accuracy, improved efficiency in material handling and drug product manufacture, and adherence to specifications).

While the last decade has seen a general shift toward direct compression and dry methods of granulation, wet granulation is still frequently used in the pharmaceutical industry (McCormick, 2005). It is particularly effective in instances where uniform distribution of a minor constituent (e.g. active, binder, wetting agent, pH modifier, antioxidant, etc.) within the bulk of the formulation is critical to drug product's performance. For example, when the drug load in the granulation is extremely low (<5%, w/w), uniform distribution of active is critical to ensure content uniformity. On the other hand, when the drug load in the granulation is extremely high (>80%, w/w), coating the drug particles with the binder is critical both in tablet manufacture and performance.

The various methods of wet granulation are classified based on the level of shear and impact that the particles experience as they are agglomerated in a wet state. In an ascending order of agitation forces, these include fluid bed granulation, rotogranulation, high-shear granulation and twin-screw extrusion. Enhanced spreading of liquid binder on the particles to be agglomerated is sometimes desirable, that led to techniques involving spray and foam granulation. While the choice of methods is often driven by the internal expertise within each organization, gaps do exist in choosing methods based on the material properties of active and the binder. With this as the larger goal, the present study attempts to correlate the material properties of actives to the processibility and performance of granulations produced by the high-shear wet technique.

The current industrial practice to gain knowledge about a wet-granulated product in the early stages of drug development is to

* Corresponding author. Tel.: +1 732 227 6425; fax: +1 732 227 3990.
*E-mail address:* chandra.vema-varapu@bms.com (C. Vemavarapu).

0378-5173/$ – see front matter © 2009 Elsevier B.V. All rights reserved.
doi:10.1016/j.ijpharm.2009.03.014

rely largely on miniaturization of equipment. Subsequent 'process work' involving optimization, scale-up, ruggedness and justification, all employ experimental designs for each active to investigate the process on a case-by-case basis. Development of physical models, on the other hand, use experimental data from one composition with no regard to the effect of materials on the process. While the effect of process on materials is investigated to a great detail in both stochastic and physical forms of modeling, very little attention has been paid vice versa. In the authors' view, this disconnect between the theoretical models and the industrial practice can be bridged by using materials as probes to understand wet granulation at a micro-scale. The purpose of the present work is therefore to examine the relationship between the physical properties of an active pharmaceutical ingredient (API) and its behavior during high-shear wet granulation. Where such correlations are developed, design of suitable process/conditions tailored to the properties of the active is achievable—an essential component of the quality by design (QbD) initiative. Alternatively, allowable variation in the properties of staring material can be defined to produce a robust wet granulated product.

Various properties of materials to be wet granulated were chosen based on their perceived role in the different stages of high-shear wet granulation, including wetting and nucleation; coalescence, consolidation and growth, and attrition of wet agglomerates. The framework for delineation of above rate processes, together with current understanding of each of these rate events are covered in the excellent reviews of Iveson et al. (2001), Litster et al. (2004), and Ennis (2005). Based on such a framework, the material properties evaluated in this study include: aqueous solubility ($S$), wettability (contact angle with water, CA), water holding capacity (equilibrium wt. gain at 97% RH, WHC), particle size (PS) and BET surface area (SA). While published evidence exists on the effects of some of the abovementioned material attributes, such studies are characteristically single-factor/univariate in design without adequate control over factors outside of the design. As a result, it is difficult to delineate the main effects, often contributing to the inconsistencies between studies (e.g. effect of particle size in Badawy and Hussain, 2004; effects of solubility/contact angle/surface tension summarized in Iveson et al., 2001). In contrast, the present study utilizes a number of materials to probe the effects in a multi-factorial design, allowing for delineation of not only the main effects but also the interactions between various factors. A series of actives and excipients were thus chosen to provide a large spread in the combinations of the abovementioned properties (Table 1). The influence of these variables on the processibility and performance of the granulation was evaluated by monitoring such responses as granule growth, compactability and flow changes upon wet granulation.

## 2. Materials and methods

### 2.1. Criteria for material selection

A primary criterion used in the selection of materials was to cover a large design space with the variables of interest. To serve this purpose, actives and also excipients with a wide range of molecular weights were included (Table 1). On the other hand, the choice of materials was restricted by the fact that identical process conditions are to be used in this study, while yielding workable granulations. For example, materials with aqueous solubility values in excess of 200 mg/ml were excluded, such that a common level of water for granulation could be used for all the materials. Since the primary intent was to investigate the effect of materials on the granulation process, care was taken to ensure that the physical form of the materials is unaltered during and after wet granulation. Accordingly, salts and molecules known to undergo form conversions were mostly excluded in this study.

### 2.2. Determination of input material properties

#### 2.2.1. Solubility

The aqueous solubility values of the various test materials were obtained from literature (Merck Index, Analytical Profiles of Drug Substances and Excipients, USP). Where the solubility of any material is only qualitatively described, USP definitions were used to

**Table 1**
List of test compounds and associated material properties.

| | Model compound | $H_2O$ solubility, mg/ml at pH 5–7 | Wettability, Contact angle (°) | $H_2O$ holding capacity, wt.% gain at 97% RH | Particle size | | Surface area, BET ($m^2/g$) | Pore vol., $cm^3/g$ (1.7–300 nm) |
|---|---|---|---|---|---|---|---|---|
| | | | | | D(3,2) μm | D90/D10 | | |
| 1 | Acetaminophen, USP | 14.300 | 77 | 0.20 | 12 | 25.9 | 0.2698 | 2.21E-04 |
| 2 | Aspirin, USP | 3.300 | 87 | 0.19 | 452 | 3.8 | 0.0189 | – |
| 3 | Aspirin-REPEAT | 3.300 | 87 | 0.19 | 452 | 3.8 | 0.0189 | – |
| 4 | Avicel-PH101 | 0.100 | 73 | 16.59 | 41 | 6.4 | 1.1596 | 2.89E-03 |
| 5 | Avicel-PH102 | 0.100 | 73 | 16.57 | 70 | 6.0 | 1.0193 | 2.47E-03 |
| 6 | Avicel-PH200 | 0.100 | 73 | 10.97 | 124 | 4.6 | 1.1960 | 2.95E-03 |
| 7 | BMS-A | 0.009 | 132 | 0.15 | 2 | 19.6 | 5.2573 | 1.10E-02 |
| 8 | BMS-B | 0.016 | 145 | 2.08 | 5 | 12.2 | 0.4621 | 1.21E-03 |
| 9 | BMS-C | 0.010 | 136 | 0.39 | 4 | 14.1 | 0.9872 | 1.60E-03 |
| 10 | BMS-D | 0.003 | 128 | 0.33 | 4 | 10.7 | 0.3193 | 5.48E-04 |
| 11 | Caffeine anhydrous, USP | 22.000 | 41 | 7.46 | 7 | 54.5 | 0.9104 | 3.12E-03 |
| 12 | Calcium carbonate USP, light powder | 0.100 | 59 | 1.86 | 1 | 9.5 | 6.1330 | 2.70E-02 |
| 13 | Dibasic calcium phosphate anhydrous, USP | 0.320 | 43 | 0.59 | 5 | 15.6 | 2.3976 | 9.94E-03 |
| 14 | Griseofulvin | 0.009 | 136 | 0.17 | 11 | 14.2 | 1.9069 | 5.86E-03 |
| 15 | BMS-E | 0.010 | 146 | 0.63 | 3 | 11.6 | 2.3296 | 4.04E-03 |
| 16 | BMS-E-REPEAT | 0.010 | 146 | 0.63 | 3 | 11.6 | 2.3296 | 4.04E-03 |
| 17 | Isoniazid | 140.300 | 0 | 0.18 | 72 | 12.1 | 0.0455 | |
| 18 | Lactose anhydrous DC NF | 200.000 | 0 | 7.02 | 28 | 27.0 | 0.4550 | 8.41E-04 |
| 19 | Lactose monohydrate SD dry | 200.000 | 0 | 1.97 | 85 | 3.4 | 0.3846 | 1.05E-03 |
| 20 | Mannitol 60 | 182.000 | 0 | 0.83 | 23 | 30.0 | 0.2626 | 3.91E-04 |
| 21 | Mannitol granular USP | 182.000 | 0 | 3.98 | 252 | 3.8 | 0.5911 | 1.84E-03 |
| 22 | Pregelatinized starch | 15.000 | 85 | 30.48 | 19 | 12.7 | 0.3442 | 6.04E-04 |
| 23 | Salicylic acid, USP | 2.240 | 136 | 1.20 | 15 | 9.7 | 0.1965 | 2.34E-04 |
| 24 | Starch, maize | 1.800 | 86 | 26.98 | 7 | 2.7 | 0.5082 | 8.26E-04 |
| 25 | Theophylline anhydrous, USP | 7.300 | 70 | 10.50 | 15 | 28.3 | 0.6065 | 1.19E-03 |

make numerical assignments. For the purpose of this study, it should be noted that the accuracy of solubility values is limited to logarithmic units of mg/ml. Accordingly, the conclusions from the study will be subject to solubility differences in excess of the predetermined level of accuracy.

*2.2.2. Contact angle*

Advancing contact angle, $\theta$ of test materials against water was determined using either the Washburn technique ($\theta < 90^\circ$; Kruss Tensiometer, K12-MK5, Kruss GmbH, NC) or the goniometer ($\theta > 90^\circ$; Drop shape analysis system-DSA10-MK2, Kruss GmbH, NC). Using the goniometer, while contact angles are recorded in a real time from 0.08 to 30 s, the values reported here are equilibrium contact angles at 30 s. Since the compaction of materials at loads such as 4–5 kN was found to alter the surfaces and therefore the contact angles, the method employed here was to gently press the powder bed between two glass slides without application of much shear or normal force. This method was particularly effective in materials with CA >90° where drop penetration is not very rapid. Highly soluble materials that instantly dissolved upon contact with water disallowed measurement with either of the techniques and were therefore arbitrarily assigned a value of 0°.

*2.2.3. Water holding capacity*

The water holding capacity of various test materials at room temperature ($T = 21\,^\circ$C) was gravimetrically determined by placing 150 mg of solid in a desiccator maintained at 97% relative humidity (RH) using saturated $K_2SO_4$ solution and recording the weight gain at the end of 5, 6 and 7 days. Except for materials that deliquesced, no weight change was observed past 5 days. Percentage water uptake relative to the dry weight of materials was used to represent WHC in this study.

*2.2.4. Particle size*

Size analysis of dry powders was performed using laser diffraction (LD) technique employing laser light source ($\lambda = 632.8$ nm) and appropriate lenses (R2, R4, R5 and R7) on Sympatec® (Helos and Vibri modules, Sympatec, NJ). The air pressure to disperse the powders without any significant attrition was determined following a pressure titration in the range 0.5–5 bar (six points). After determination of the appropriate feed rate/obscurance, dispersion pressure and the size of the lens, three independent measurements were made and the reproducibility between measurements tested. Typical variation between measurements expressed as mean %R.S.D. in D10, D50 and D90 were 3.2, 2.3 and 4.1% respectively. Of the several statistics generated from the data inversion of diffraction angle/intensity to particle size, D[3,2] and D90/D10 were used respectively to represent the mean particle size and width of distribution.

*2.2.5. Nitrogen adsorption*

The surface area for the entire sample was determined using nitrogen adsorption technique by Gemini™ surface area analyzer (2380 V-series Micromeritics, GA). The sample (1.0–1.5 g) was degassed by nitrogen flow at 55 °C overnight (~8 h) using Vac Prep™ 061 (Micromeritics, GA). The amount of nitrogen adsorbed was determined at partial nitrogen pressure ($P/P_0$) ranging between 0.05 and 0.30. Surface area was determined by Gemini software using the Brunauer–Emmett–Teller's (BET) calculation for the nitrogen data in the $P/P_0$ range from 0.05 to 0.3. The goodness of fit to BET model is established in all materials ($r^2 > 0.99$), excepting two (aspirin and isoniazid, see Table 1) whose BET areas were found to approach the lower limit of measurement. The $r^2$ values for the BET model-fitted linears of aspirin and isoniazid were respectively 0.68 and 0.76.

*2.2.6. Nitrogen condensation*

Pore volumes of various materials were determined by following condensation of nitrogen (Gemini™ 2380 V, Micromeritics, GA) as a function of partial nitrogen pressure ($P/P_0$) between 0.30 and 0.98. The pressure at which nitrogen condenses in the pores is directly proportional to their size, as dictated by Kelvin equation. Following this principle, the BJH cumulative volume of pores (after Barrett, Joyner and Halenda) (Webb et al., 1997) with width between 1.7 and 300 nm was calculated using Gemini software.

*2.2.7. Preblend compactability*

'Preblend' (as will be described in Section 2.3) is identical in composition to the final granulation, but one that is not subjected to the wet granulation process. Changes as a result of wet granulation are evaluated in this study by comparing the properties of granulation (final) to that of the preblend (initial). Using 3/8 in. round standard flat-faced tooling, tabletting of preblends was simulated using EHS simulator (Huxley Bertram Engineering Ltd., UK). The die is manually filled with 300 mg of powder blend and tablets compressed at five different compression forces (range 5–30 kN). During this test, forces (compression, ejection) and displacement experienced by punches are recorded. Offline measurements on tablets include weight, thickness and hardness. Using this data, a plot is generated between tablet tensile strength ($y$) and compaction pressure ($x$) and the slope of the fitted linear is reported as 'compactability'.

*2.2.8. Preblend flow*

Flow of preblends was determined using Flodex tester (Model-211, Hanson Research, CA), wherein 30 g of test material is loaded onto a sample plate (with a fixed aperture) using a funnel. After 30 s, the aperture on this plate is opened and the powder flow through this aperture is examined. The minimum diameter of aperture in millimeters that allows the flow of material from the plate (unassisted) is reported as the Flodex number. Accordingly, smaller Flodex numbers represent better flow and vice versa.

*2.3. High-shear wet granulation*

Identical composition and process conditions were used to wet granulate various test materials, to be able to make direct comparisons between the responses. The template composition evaluated in this study contains 70% Test Compound + 26% Avicel-PH102 + 4% HPC-EXF (w/w). Process conditions for high-shear wet granulation include: batch size = 150 g, granulator = 1 L Diosna™ Bottom Driven mixer (P1-6, Diosna Dierks & Söhne, GmbH), impeller speed = 600 rpm (tip speed = 4.8 m/s), chopper speed = 2000 rpm, water for granulation = 30% of dry weight, $H_2O$ addition rate = 22.5 g/min, spray nozzle = Schlick hollow cone (aperture = 0.4 mm, spray angle = 30°, #10347, Dusen-Schlick GmbH), wet-massing time = 30 s. The level of water for granulation was determined based on preliminary runs on materials at extreme ends of solubility range. Detailed processing steps include screening the materials (#18-mesh for test compound and Avicel; #30-mesh for HPC) and dry mixing the components for 2 min. A portion of this sample (called preblend) was removed for testing the properties of blend prior to wet granulation. This was followed by the addition of water and subsequent wet-massing. The wet granulation was then tray dried in an oven at $55 \pm 5\,^\circ$C for 8 h, at the end of which the moisture content was recorded by loss on drying (HR73-P Halogen moisture analyzer, Mettler-Toledo, Inc., OH). The final LOD values of the various granulations ranged between 0.9 and 5.9% and were found to have a linear relationship with the WHC values of the respective test materials.

### 2.4. Response measurements/determination of output material properties

#### 2.4.1. Percent oversize (>1.4 mm)

Using a #14-mesh sieve, granulation that was larger than 1.4 mm was separated from the bulk and the percentage of total mass was reported as oversize. Granulation that passed through #14-mesh was recovered and used for the tests described below.

#### 2.4.2. Granule growth ratio (LD/Sieve Analysis)

Granule size was measured using the same technique and equipment that was employed for starting materials (Section 2.2). In case of granulations, dispersing air pressure (Sympatec®, Gradis and Rodos/Vibri modules used) was not used in a majority of cases where granule flow/dispersion of granulation into the path of laser light was determined to be good. Following similar data treatment as before, the D[3,2] and D90/D10 of granulations were obtained. Granule growth ratio is defined as the ratio of D[3,2] of the granulation to that of the test material. The D[3,2] values of granulations obtained from LD measurements were checked against the geometric mean diameter values from sieve analysis (Allen Bradley Sonic Sifter, Milwaukee, WI) to ensure that no artifacts are derived from the measurement techniques. Except for two materials that blinded the screens during sieve analysis, the correlation between particle size data derived from LD and Sieve analysis was found to be good ($R^2 = 0.92$).

#### 2.4.3. Compactability ratio (ESH compaction simulator)

Compactability of the granulations was determined using the same procedure described in Section 2.2. Compactability ratio is defined as the ratio of 'compactability' of the granulation to that of the preblend.

#### 2.4.4. Flow ratio

Flodex numbers for the granulations are determined as described in Section 2.2. Flow ratio is defined as the ratio of Flodex number of the granulation to that of the preblend. Other numbers such as the difference between the Flodex values prior to and after wet granulation or the percentage difference from initial could also be used to represent the change in flow. Selection of ratio of granulation to preblend Flodex values for data analysis was made to have consistency among the performance indicating responses. However, it should be realized that smaller flow ratio represents larger improvement in flow.

### 2.5. Data analysis and interpretation

The present study involves fitting statistical models to explain five responses based on seven factors (Table 1). Determination of correlations between the various factors was therefore necessary to allow reduction in the model size, as well as the number of experiments. Since a linear correlation was observed between porosity and BET surface area, the former was not used in regression analysis. A total of six independent factors were thus chosen for model fitting. Mathematical transformation of this data was subsequently performed using SAS-JMP software (Release 6.0.3, SAS Institute Inc.) in order to attain a normal distribution of the population selected. Such data transformation was deemed important, so that the population can be characterized by a mean and variance (Bland and Altman, 1996). Where applicable, the response variables (Table 2) were similarly transformed into normal probability distributions. The goodness of fit of the various distributions prior to and after the transformation was tested using Shapiro-Wilk W test. Table 3 summarizes the applied transformations to all the $x$- and $y$-terms used in subsequent regression analysis.

Model fitting was performed using stepwise regression involving six factors (main effects and two-way interactions) for each of the five responses and the significant relationships ($p < 0.05$) identified. All the data analyses were performed using SAS-JMP software (Release 6.0.3, SAS Institute Inc.). Given the size of this statistical study and the inherent constraints in its design (Section 2.1), the physical interpretation of data (Section 3) will be limited to only the main effects. Explanation of the physical effects in this manuscript relied largely on the prevailing theories on wet granulation, excel-

**Table 2**
Summary of responses.

| | Model compound | % LOD | % Oversize, (>1.4 mm) | Flodex flow number, mm | | Compactability, KPa/MPa | | D(3,2) μm | D90/D10 | Growth ratio |
|---|---|---|---|---|---|---|---|---|---|---|
| | | | | Preblend | Granulation | Preblend | Granulation | | | |
| 1 | Acetaminophen, USP | 0.85 | 20.2 | 26 | 5 | 1.73 | 3.01 | 272 | 3.6 | 23.1 |
| 2 | Aspirin, USP | 0.67 | 68.0 | 10 | 8 | 2.52 | 2.23 | 989 | 2.3 | 2.2 |
| 3 | Aspirin-REPEAT | 0.76 | 74.1 | 9 | 14 | 2.86 | 2.39 | 840 | 2.4 | 1.9 |
| 4 | Avicel-PH101 | 2.71 | 0.0 | 14 | 5 | 8.70 | 7.47 | 62 | 5.5 | 1.5 |
| 5 | Avicel-PH102 | 3.36 | 0.1 | 5 | 5 | 10.52 | 8.27 | 101 | 4.9 | 1.4 |
| 6 | Avicel-PH200 | 2.98 | 0.3 | 4 | 4 | 7.03 | 6.48 | 144 | 4.2 | 1.2 |
| 7 | BMS-A | 0.85 | 2.7 | 32 | 24 | 2.40 | 5.67 | 21 | 51.5 | 13.5 |
| 8 | BMS-B | 0.70 | 12.9 | 30 | 6 | 1.85 | 3.14 | 158 | 5.3 | 33.2 |
| 9 | BMS-C | 0.90 | 11.0 | 30 | 6 | 2.76 | 5.77 | 135 | 7.6 | 33.9 |
| 10 | BMS-D | 0.90 | 13.4 | 24 | 4 | 3.64 | 5.28 | 165 | 4.8 | 44.8 |
| 11 | Caffeine anhydrous, USP | 0.89 | 16.8 | 24 | 8 | 6.41 | 7.68 | 191 | 8.1 | 26.2 |
| 12 | Calcium carbonate USP, light powder | 0.96 | 4.0 | >32 | 26 | 5.67 | 5.39 | 161 | 3.5 | 114.7 |
| 13 | Dibasic calcium phosphate anhydrous, USP | 1.06 | 3.3 | 14 | 4 | 8.79 | 9.07 | 86 | 5.9 | 19.1 |
| 14 | Griseofulvin | 0.91 | 15.0 | 32 | 4 | 7.33 | 8.68 | 150 | 6.1 | 13.6 |
| 15 | BMS-E | 1.03 | 10.2 | >32 | 30 | 2.81 | 6.24 | 17 | 36.4 | 5.8 |
| 16 | BMS-E-REPEAT | 0.99 | 5.2 | >32 | 26 | 2.81 | 6.77 | 14 | 39.9 | 4.7 |
| 17 | Isoniazid | 0.70 | 96.8 | 14 | – | 2.35 | 3.13 | 1400 | 3.0 | 19.5 |
| 18 | Lactose anhydrous DC NF | 1.13 | 16.6 | 14 | 5 | 10.69 | 8.01 | 348 | 3.1 | 12.3 |
| 19 | Lactose monohydrate SD dry | 0.98 | 26.7 | 4 | 6 | 10.79 | 9.08 | 418 | 3.5 | 4.9 |
| 20 | Mannitol 60 | 0.74 | 96.3 | 18 | – | 4.47 | 5.79 | 1400 | 3.0 | 60.4 |
| 21 | Mannitol granular USP | 0.79 | 30.4 | 8 | 6 | 4.57 | 5.17 | 665 | 2.9 | 2.6 |
| 22 | Pregelatinized starch | 4.63 | 35.3 | 16 | 8 | 3.89 | 2.76 | 283 | 7.1 | 14.7 |
| 23 | Salicylic acid, USP | – | 15.5 | 30 | 14 | 3.30 | 4.14 | 159 | 4.1 | 10.3 |
| 24 | Starch, maize | 5.92 | 7.5 | 26 | 12 | 3.85 | 0.86 | 111 | 10.7 | 15.2 |
| 25 | Theophylline anhydrous, USP | 1.12 | 10.2 | 30 | 8 | 6.00 | 7.78 | 176 | 9.6 | 12.0 |

**Table 3**
List of factors and responses.

| Factors | | Responses | |
|---|---|---|---|
| | Transformation | | Transformation |
| Water solubility | log | Compactability ratio | None |
| Wettability | None | Flow ratio | log |
| Water holding capacity | log | Granule growth ratio | log |
| Particle size—D(3,2) | log | Width of granule PSD—D90/D10 | log |
| Width of particle PSD—D90/D10 | log | | |
| Surface area | Cube root | Percent oversize | Square root |

**Table 4**
Statistical summary of fit-controlled growth.

| log(granule growth ratio) | | | | |
|---|---|---|---|---|
| Summary of fit | | Parameter estimates | | |
| | | Term | Estimate | Prob > \|t\| |
| RSquare | 0.78 | Intercept | 3.32 | <0.0001 |
| RSquare adj | 0.75 | Contact angle | 0.00 | 0.0008 |
| Root mean square error | 0.27 | log(D3,2) | −0.97 | <0.0001 |
| Mean of response | 1.01 | Cube root (BET) | −0.79 | 0.0005 |
| Observations (or sum wgts.) | 25 | | | |

lent treatises of which can be found in the references cited here (Iveson et al., 2001; Litster et al., 2004; Ennis, 2005).

The output from the regression analysis using SAS-JMP is summarized in two different formats, namely (a) leverage plots (Figs. 1–5) and (b) summary of fit (Tables 4–8). The leverage plot for the linear effect in a simple regression is the same as the traditional plot of actual response values ($y$) and the regressor ($x$). The distance from a point to the line of fit shows the actual residual. The distance from the point to the horizontal line of the mean shows what the residual error would be without the effect in the model. In other words, the mean line in this leverage plot represents the model where the hypothesized value of the parameter ($x$) is constrained to zero. Alternatively, adjusted $r^2$ values of the whole model, as well as the parameter estimates and their significance, ($p$-values) are summarized in Tables 4–8. Using these terms, it is possible to calculate the response ($y$) by plugging in the $x$-terms, to the extent this statistical model is valid.

## 3. Results and discussion

### 3.1. Controlled growth

Controlled or steady growth of materials is a desirable attribute in wet granulation process as it is expected to provide robustness to the drug product while accommodating typically encountered variances in the material and process attributes. It is mapped as a region on the two-dimensional plot of Stokes granule deformation number and granule pore saturation, optimal levels of both of which contribute to fruitful coalescence, consolidation and growth (Ennis, 2005; Iveson et al., 2001). Stokes deformation number ($\rho_g U_c^2/2Y_g$) derives from balancing kinetic energy with plastic deformation of granules and is therefore a measure of growth by coalescence. Granule pore saturation (Eq. (1)), on the other hand, quantifies the portion of pores within a granule that is filled with liquid. While taking into account both the volume of available pores as well as the liquid volume, it is a measure of the thickness of liquid film around the granules.

$$\text{pore saturation}, s = \frac{w\rho_s(1-\varepsilon)}{\rho_l \varepsilon} \quad (1)$$

For the purposes of this study, controlled growth is quantified by the increase in the D[3,2] value of the powder blend upon wet granulation without over-growth to sizes greater than 1.4 mm. Regression analysis of the granule growth data yielded three statistically significant terms namely CA, PS and SA. Refer to Table 4 for the summary of statistical analysis and Fig. 1 for the trends. As can be seen from Fig. 1, granule growth ratio is low in materials with high contact angles. This is expected to be a manifestation of (a) slow nucleation and (b) low strength of wet granule in materials with high contact angles. Nucleation event relies on wetting to be thermodynamically favorable (positive spreading coefficient, Eq. (2)), and for drop penetration (Eq. (3)) to occur instantaneously. The contribution from the latter may be minimal in high-shear process employing water for granulation due to the efficient mechanical dispersion of water droplets. As can be seen from Eqs. (1) and (2) (Iveson et al., 2001; Ennis, 2005), both these are impeded when contact angle between the liquid and the solid particles is high.

$$\text{work of spreading (LS)}: \quad W_{CL} - W_A = \lambda_{lv}(\cos\theta - 1) \quad (2)$$

$$\text{drop penetration}: \ \text{tp} = 1.35 \left[\frac{V_d^{2/3}}{\varepsilon_{\text{eff}}^2}\right]\left[\frac{\mu}{R_{\text{eff}}\gamma_{lv}}\cos\theta\right] \quad (3)$$

Additionally, the static strength of the wet granule is also lowered at high contact angles Rumpf Eq. (3).

$$\text{static strength of liquid bound granules (Rumpf)}: \ \sigma_T = \text{SC}\left[\frac{1-\varepsilon}{\varepsilon}\right]\left[\frac{\lambda_{lv}\cos\theta}{d_p}\right] \quad (4)$$

Once formed, the wet granule should withstand the high shear and impact forces generated in the mixer. Lack of such strength results in breakage of wet granules, thus reducing the eventual

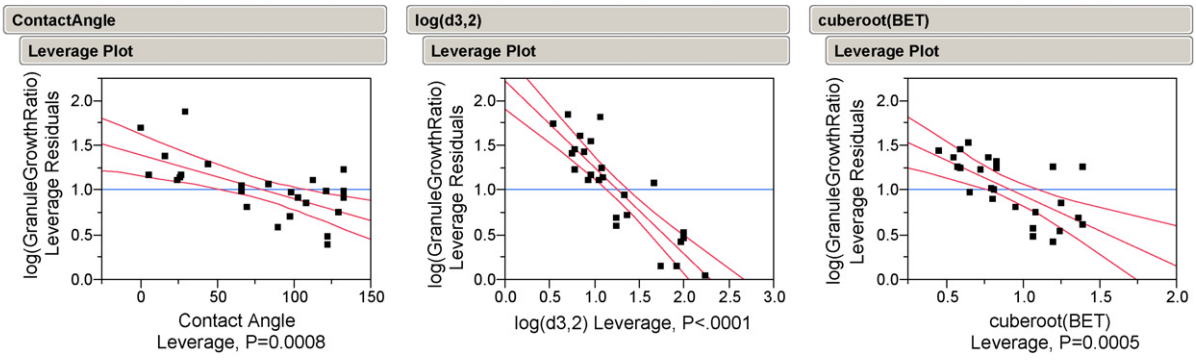


**Fig. 1.** Significant material properties affecting controlled growth.

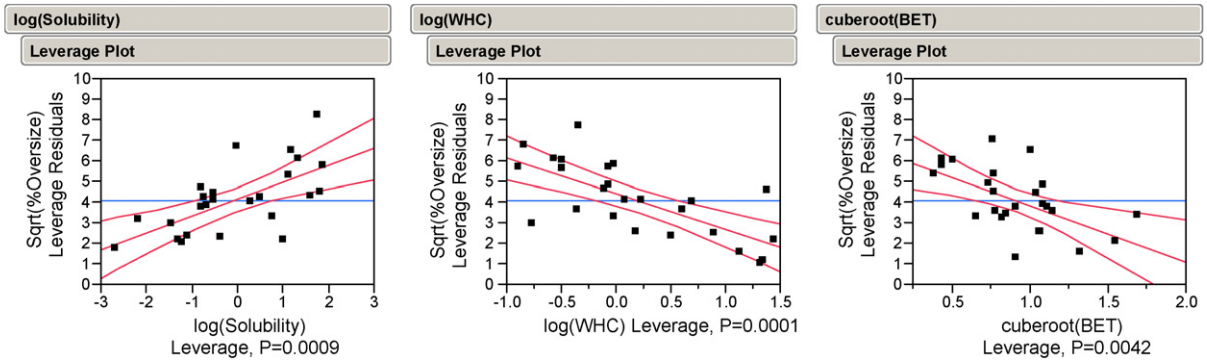


**Fig. 2.** Significant material properties affecting uncontrolled growth.

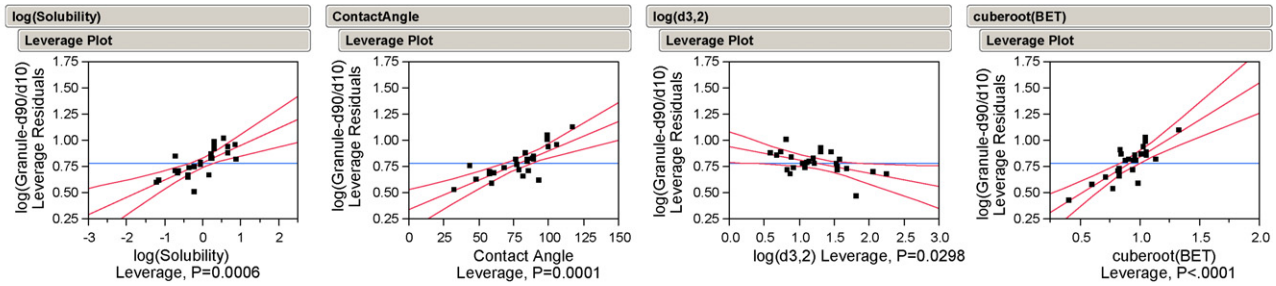


**Fig. 3.** Significant material properties affecting width of granule size distribution.

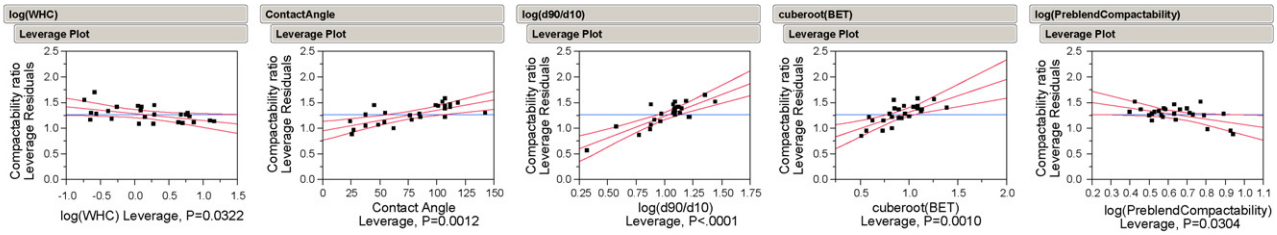


**Fig. 4.** Significant material properties affecting compactability ratio.

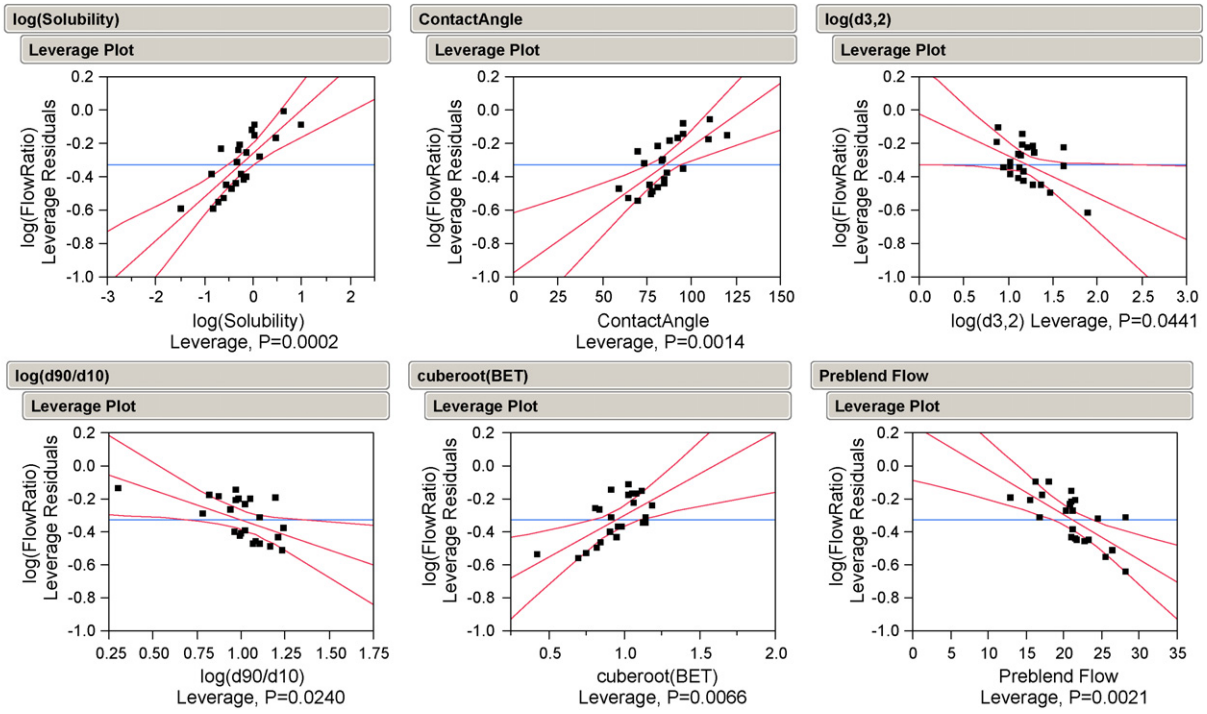


**Fig. 5.** Significant material properties affecting flow ratio.

**Table 5**
Statistical summary of fit-uncontrolled growth.

| Sqrt. (%oversize) | | | | |
|---|---|---|---|---|
| Summary of fit | | Parameter estimates | | |
| | | Term | Estimate | Prob > \|t\| |
| RSquare | 0.79 | Intercept | 6.94 | <0.0001 |
| RSquare adj | 0.76 | log(solubility) | 0.82 | 0.0009 |
| Root mean square error | 1.34 | log(WHC) | −1.74 | 0.0001 |
| Mean of response | 4.08 | Cube root (BET) | −2.74 | 0.0042 |
| Observations (or sum wgts.) | 25 | | | |

**Table 6**
Statistical summary of fit-width of granule size distribution.

| log(D90/D10) of granule | | | | |
|---|---|---|---|---|
| Summary of fit | | Parameter estimates | | |
| | | Term | Estimate | Prob > \|t\| |
| RSquare | 0.94 | Intercept | 0.08 | 0.729 |
| RSquare adj | 0.91 | log(solubility) | 0.17 | 0.0006 |
| Root mean square error | 0.11 | Contact angle | 0.01 | 0.0001 |
| Mean of response | 0.78 | log(D3,2) | −0.13 | 0.0298 |
| Observations (or sum wgts.) | 25 | Cube root (BET) | 0.71 | <.0001 |
| | | (log(solubility) + 0.05883) × (contact angle − 78.36) | 0.00 | 0.0009 |
| | | (log(solubility) + 0.05883) × (cube root (BET) − 0.9111) | 0.94 | <0.0001 |
| | | (Contact angle − 78.36) × (cube root (BET) − 0.9111) | 0.03 | <0.0001 |
| | | (log(D3,2) − 1.24536) × (cube root (BET) − 0.9111) | −0.43 | 0.0029 |

growth ratio. These results of the negative influence of contact angle on granule growth are also in agreement with the published literature (Jaiyeoba and Spring, 1980; Iveson et al., 2001).

Granule growth ratio was found to be low in materials with large initial particle size. This can be explained based on the fact that the strength of wet granule is low when the constituent particle size is large (Eq. (3)). The density of interparticle contacts is low and as a result, the frictional resistance that contributes to the strength of wet granules is also low (Iveson et al., 2001). Accordingly, the extent of wet granule breakage is high in composites made of large particles, leading to the reduced granule growth seen in large PS materials. An inverse relationship between the initial particle size and granule growth was also reported in the earlier published work (Badawy and Hussain, 2004).

**Table 7**
Statistical summary of fit-compactability ratio.

| Compactability ratio | | | | |
|---|---|---|---|---|
| Summary of fit | | Parameter estimates | | |
| | | Term | Estimate | Prob > \|t\| |
| RSquare | 0.94 | Intercept | −0.39 | 0.3422 |
| RSquare adj | 0.91 | log(WHC) | −0.14 | 0.0322 |
| Root mean square error | 0.17 | Contact angle | 0.00 | 0.0012 |
| Mean of response | 1.26 | log(D3,2) | 0.11 | 0.2746 |
| Observations (or sum wgts.) | 25 | log(D90/D10) | 0.85 | <0.0001 |
| | | Cube root (BET) | 0.64 | 0.001 |
| | | log(preblend compactability) | −0.54 | 0.0304 |
| | | (log(WHC) − 0.18427) × (cube root (BET) − 0.9111) | 0.78 | 0.0055 |
| | | (Contact angle − 78.36) × (log(D3,2) − 1.24536) | −0.01 | 0.0005 |
| | | (Cube root (BET) − 0.9111) × (log(preblend compactability) − 0.64147) | −1.73 | 0.0396 |

**Table 8**
Statistical summary of fit-flow ratio.

| Log (flow ratio) | | | | |
|---|---|---|---|---|
| Summary of fit | | Parameter estimates | | |
| | | Term | Estimate | Prob > \|t\| |
| RSquare | 0.89 | Intercept | −0.37 | 0.2653 |
| RSquare adj | 0.82 | log(solubility) | 0.26 | 0.0002 |
| Root mean square error | 0.13 | Contact angle | 0.01 | 0.0014 |
| Mean of response | −0.33 | log(D3,2) | −0.25 | 0.0441 |
| Observations (or sum wgts.) | 23 | log(D90/D10) | −0.36 | 0.024 |
| | | Cube root (BET) | 0.50 | 0.0066 |
| | | Preblend flow | −0.03 | 0.0021 |
| | | (Contact angle − 85.1739) × (log(D90/D10) − 1.00418) | −0.01 | 0.04 |
| | | (log(D3,2) − 1.21356) × (preblend flow − 21.1739) | −0.04 | 0.0001 |

It is noteworthy to mention that due to the lack of correlation between particle size$^{-1}$ and BET surface area, inclusion of both terms in statistical analysis was necessary. Where both terms are found significant, BET surface area is primarily construed as the internal area (intraparticle porosity) with additional contribution of surface irregularities. Such an assumption is validated by the linear relationship found between porosity and BET area, as determined by $N_2$ condensation and adsorption. As can be seen from Fig. 1, granule growth was found to decrease as BET area increased. The penetration of water into the pores of the primary particles makes less of it available at the particle surface (↓ liquid film thickness), hence reducing the chances of coalescence and growth. This can be also explained based on reduced granule pore saturation (Eq. (4)) when the BET area is high, as a result of which growth is hindered (Iveson et al., 2001).

### 3.2. Uncontrolled growth

Uncontrolled or rapid granule growth is undesirable as it renders the drug product to be highly sensitive to even moderate changes in formulation or process. High percent oversize is indicative of uncontrolled granule coalescence and growth. Poor liquid distribution can also contribute to high oversize values. Regression analysis of the percent oversize data yielded three statistically significant terms namely S, WHC and SA. Refer to Table 5 for the summary of statistical analysis and Fig. 2 for the trends.

As expected, granule growth was found to be uncontrolled in highly soluble compositions. As materials dissolve, the liquid-to-solid ratio and therefore pore saturation becomes high (Eq. (4)) which shifts the growth phase to an uncontrolled region (Iveson et al., 2001). Increased viscosity of liquid film upon dissolution of materials also contributes to an increase in the dynamic strength of granules, resisting any breakage (Eq. (5), Iveson et al., 2001).

$$\text{dynamic strength of liquid bridges within granules : Fv} = \left(\frac{3\pi\mu r_p^2}{2h}\right)\left(\frac{dh}{dt}\right) \quad (5)$$

Percent oversize data also indicated that granule growth is uncontrolled in materials with low WHC. Since materials with high WHC tend to sorb water into their particles, it can be expected that at a given water level, the thickness of liquid film around particles is high when WHC is low. In a similar vein, materials with low BET area exhibited high percent oversize values. Both these results are consistent with the relationship proposed above, linking high pore saturation to uncontrolled growth.

### 3.3. Width of granule size distribution

Analysis of the width of granule size distribution is important as it provides useful information about the granulation events, in addition to what a 'mean size' depicts. Further, this has significant influence on aspects such as segregation, flow and compressibility of the granulations. While several statistics can be used to represent the 'distribution width' (FWHM, d90/d25, [d90-d10]/d50, StdDev), the present study employs D90/D10 value from volume-based distribution (laser diffraction data). In principle, wide size distributions are known to result from (a) improper liquid distribution and (b) weak or fragile granule formation. Regression analysis of D90/D10 of granulations identified four significant factors, namely S, CA, PS and SA. Refer to Table 6 for the summary of statistical analysis and Fig. 3 for the trends.

As can be seen from Fig. 3, the higher the solubility of the test material, the broader is the width of granule distribution. This is believed to originate from the higher tendency of high-solubility materials for uncontrolled growth (Section 3.1). Also, increased viscosity of the liquid upon dissolution of soluble components could occur, that hinders uniform liquid distribution, yielding 'lumps' and ungranulated masses. It can also be argued that reprecipitation of solids at granule surface after migration and subsequent evaporation of water could cause attrition of active from dried granules. This, in turn results in a wide distribution in the granule sizes. Similar arguments were presented in explaining the segregation of soluble materials during and after wet granulation (Iveson et al., 2001).

The width of granule distribution was also found to be high when the contact angle and BET area of the test materials are high, and the initial particle size is low. While inadequate liquid wetting and distribution can be implicated in the observed effects of CA, it is only a hypothesis with no ready evidence from literature or substantiation from studies using other water levels. Lastly, a useful contribution from evaluating the 'width' of granule distributions is that, it formed a basis for the interpretation of flow data (Section 3.5).

### 3.4. Compactability ratio

Change in compactability upon wet granulation is a combined effect of loss in porosity and size enlargement of the constituent particles on one hand, with a concomitant increase in the bonding/plasticity of particles upon uniform application of the binder. While the former is known to decrease compactability following wet granulation, the latter enhances the compactability through activation of binder. As can be seen from Table 2, the latter mechanism is dominant than the former with the compactability ratio >1 in several compositions. While it is difficult to delineate these mechanisms affecting compactability in the present study, it is also of practical significance to connect this critical drug product attribute to the physical properties of starting materials. It was therefore included as a response indicating the 'performance' of wet granulations in the present study. Upon a preliminary evaluation of this response, it became evident that the compactability ratio was affected by the initial compactability of the preblend. The latter was therefore included in the statistical model, in addition to other terms summarized in Table 3. Regression analysis of 'compactability ratio' data resulted in several significant factors including the preblend compactability, supporting its inclusion in the model. Refer to Table 7 for the summary of statistical analysis and Fig. 4 for the trends.

The increase in compactability upon wet granulation was found to be highest in materials with low initial compactability. This result is consistent with the second mechanism mentioned above, whereby the application of a uniform binder layer enhances compactability of powders. Materials with high WHC showed least improvement in compactability upon wet granulation. This is believed to be a direct consequence of loss in intraparticle porosity following granulation, with the underlying assumption that materials with high WHC have primary particles that can be densified (e.g. celluloses, starches, and large molecules) as a result of granulation (Badawy et al., 2006).

Contact angle is another material property that was found to have a significant influence on compactability ratio. As can be seen from Fig. 4, materials with high contact angles showed largest improvement in compactability upon granulation. The effect of contact angle on compactability ratio is dual, in that the binder distribution is not perfect with difficult-to-wet materials. This should render lower compactability ratios at high contact angles. Alternatively, the extent of consolidation is low at high contact angles due to the reduced interparticle lubrication by a non-wetting liquid (Iveson and Litster, 1998). As a result, granules made from high CA materials have high porosity and thus higher compactability ratios.

Further, in instances where granule size affects compactability (typical at low granule porosity), it can be argued that high contact angle results in increased compactability ratio mediated through minimal size enlargement.

Compactability increase was found to be highest in materials with high BET area. Such an effect can readily be linked to low granule growth and wide granule size distributions, seen when BET area of starting materials is high. In addition, high BET area makes less water to be available at the particle surface. Since water acts as a lubricant in decreasing interparticle friction, the extent of consolidation is low in high BET materials, thus resulting in higher compactability ratios. Alternatively, the large internal area/porosity indicative of the high BET values of starting materials, if lost during wet granulation should have resulted in an inverse relationship. It was found in this study that the former effects are more prominent than the latter. Data on extent of consolidation of the granules as a function of initial BET area will be useful to delineate the above competing effects.

Lastly, the width of the size distribution of starting materials was also found to influence the compactability ratio. Broad initial size distributions, when wet granulated, are reported to exhibit high consolidation, wet agglomerate strength and the final granule size (Adetayo et al., 1993; Iveson et al., 2001). Contrary to our finding (Fig. 4), all the abovementioned factors support an inverse relationship between width of material PSD and compactability ratio. In fact, the reported effect of the width of material PSD on granule size was also not verified in the current study (Section 3.1). Additional data on granule porosity and binder distribution as function of PSD width of starting material will qualify this relationship and will be the subject of a future investigation.

### 3.5. Flow ratio

Improvement in flow upon granulation is expected to be a combined result of size enlargement, densification, reduction in the width of powder size distribution as well as the percentage of fines and lastly, surface modification or rounding. Flow data will therefore need to be interpreted based on the inferred effect from the abovementioned factors. Regression analysis of 'flow ratio' data resulted in six significant factors including the preblend flow, supporting its inclusion in the model. Refer Table 8 for the summary of statistical analysis and Fig. 5 for the trends. As described in Section 2.4, it should be noted here that low 'flow ratio' values indicate greater improvement in flow upon granulation.

As seen with compactability, the change in flow of materials was also dependent on the initial flow of starting materials (preblends). Data indicated that greater improvement in flow can be expected of poorly flowing blends, when wet granulated. Inclusion of this factor in the statistical model was therefore necessary such that the influence of other terms is reflected accurately.

An inverse relationship was observed between the aqueous solubility of materials and flow enhancement. This is likely derived from the fact that poorly soluble materials are typically finely milled and therefore have poor intrinsic flow properties. In addition, better flow improvement may be a manifestation of tighter granule size distributions seen when poorly soluble materials are wet granulated (Section 3.3). Similar argument holds for the effect of particle size, contact angle and BET area, all of which have shown consistent effect on the width of granule size distribution and flow improvement. Larger improvement in flow when CA and SA are low can also be attributed to the higher granule growth seen at these conditions (Section 3.1). Consistent with the effect of CA on granule porosity (Section 3.4), higher densification of low contact angle materials can also be implicated for higher flow enhancement. Lastly, flow improvement was found to be highest in materials with broader initial size distributions. By reducing the width of the size distribution, the tendency for powders to consolidate under their own weight is decreased, as a result of which the flow was improved.

## 4. Conclusions

This study illustrates the dependence of the processibility and performance of a wet granulated product on a number of intrinsic material properties. The prominent findings from this study are summarized here: (a) high solubility compounds have greater tendency for uncontrolled growth, (b) compounds with high water uptake showed reduced compactability upon wet granulation, (c) high contact angle APIs resulted in polydisperse granulations, (d) large API particles showed negative effect on granule growth, (e) increase in compactability upon wet granulation is higher in APIs with large PSD and (f) BET surface area (in addition to particle size) affects a number of granulation properties.

The basis for the selection of these properties was not only their perceived role in wet granulation, but also the availability of such data early in drug development. Findings from this study are thus useful in mapping a new material to qualitatively predict its performance in a high-shear wet granulation process. Quantitative predictions are only possible if such models are improved with additional datasets. Inclusion of relevant mechanical properties is a possibility, although limited by the availability of test methods for powders with irregular geometries. In summary, studies such as these are timely in present day dosage form development, wherein the identification and control of critical quality attributes and their sources of origin are increasingly being emphasized.

*Symbols*

| | |
|---|---|
| S | aqueous solubility |
| CA | contact angle with water |
| WHC | water holding capacity (equilibrium wt. gain at 97% RH) |
| PS | particle size |
| SA | BET surface area |
| $W_{CL}$ | work of cohesion for a liquid |
| $W_A$ | work of adhesion for an interface |
| $\gamma_{lv}$ | surface tension between solid and liquid |
| $\theta$ | solid–liquid contact angle |
| tp | total drop penetration time |
| $V_d$ | drop size |
| $\varepsilon_{eff}$ | porosity of powder bed |
| $\mu$ | liquid viscosity |
| $R_{eff}$ | effective pore radius |
| $\sigma_T$ | tensile strength of wet granule |
| $s$ | liquid pore saturation |
| $C$ | material constant (=6 for uniform spheres) |
| $\varepsilon$ | granule porosity |
| $d_p$ | surface-average particle diameter (D[3,2]) |
| $w$ | mass ratio of liquid-to-solid |
| $\rho_s$ | density of solid particles |
| $\rho_l$ | density of liquid |
| $\rho_g$ | granule density |
| $U_c$ | granule impact velocity |
| $Y_g$ | dynamic yield stress of granule |
| Fv | dynamic strength of pendular liquid bridge |
| $r_p$ | particle radius |
| $2h$ | gap between particles |
| $dh/dt$ | particle velocity |
| $t$ | time |
| D[3,2] | surface mean diameter |
| D90 | 90th percentile of PSD |
| D10 | 10th percentile of PSD |
| D25 | 25th percentile of PSD |
| FWHM | full width at half maximum |
| PSD | particle size distribution |

## Acknowledgements

The authors would like to acknowledge the support of Dr. Emil Friedman and Dr. James Bergum of Bristol-Myers Squibb Company, NJ in the statistical design and data analysis presented in this manuscript.

## References

Adetayo, A.A., Litster, J.D., Desai, M., 1993. The effect of process parameters on drum granulation of fertilizers with broad size distributions. Chem. Eng. Sci. 48, 3951–3961.

Lee, A.Y., Myerson, A.S., 2006. Particle engineering: fundamentals of particle formation and crystal growth. MRS Bull. 31, 881–886.

Badawy, S.I.F., Gray, D.B., Hussain, M.A., 2006. A study on the effect of wet granulation on microcrystalline cellulose particle structure and performance. Pharm. Res. 23, 634–640.

Badawy, S.I.F., Hussain, M.A., 2004. Effect of starting material particle size on its agglomeration behavior in high shearwet granulation. AAPS PharmSciTech 5 (Article 38) http://www.aapspharmscitech.org.

Bland, J.M., Altman, D.G., 1996. Statistics notes: transforming data. BMJ 312, 770.

Ennis, B.J., 2005. Theory of granulation: an engineering perspective. In: Parikh, D.M. (Ed.), Handbook of Pharmaceutical Granulation Technology, second edition. Taylor & Francis, NY (Chapter 2).

Iveson, S.M., Litster, J.D., 1998. Fundamental studies of granule consolidation. Part 2. Quantifying the effects of particle and binder properties. Powder Technol. 99, 243–250.

Iveson, S.M., Litster, J.D., Hapgood, K., Ennis, B.J., 2001. Nucleation, growth and breakage phenomena in agitated wet granulation processes: a review. Powder Technol. 117, 3–39.

Jaiyeoba, K.T., Spring, M.S., 1980. The granulation of ternary mixtures: the effect of the wettability of the powders. J. Pharm. Pharmacol. 32, 386–388.

Litster, J., Ennis, B., Liu, L., 2004. The Science and Engineering of Granulation Processes. Kluwer Academic Publishers, MA.

McCormick, D., 2005. Evolutions in direct compression. Pharm. Technol. (April), 52–62.

Webb, P.A., Orr, C., et al., 1997. Analytical Methods in Fine Particle Technology, first edition. Micromeritics Instrument Corporation, GA.